Impact of an Irreversibly Adsorbed Layer on Local Viscosity of Nanoconfined Polymer Melts

Tadanori Koga,[1,2,*] N. Jiang,[2] P. Gin,[2] M. K. Endoh,[2] S. Narayanan,[3] L. B. Lurio,[4] and S. K. Sinha[5]

[1]*Chemical and Molecular Engineering Program, Stony Brook University, Stony Brook, New York 11794-2275, USA*
[2]*Department of Materials Science & Engineering, Stony Brook University, Stony Brook, New York 11794-2275, USA*
[3]*Advanced Photon Source, Argonne National Laboratory, Argonne, Illinois, 60439, USA*
[4]*Department of Physics, Northern Illinois University, DeKalb, Illinois, 60115, USA*
[5]*Department of Physics, University of California San Diego, La Jolla, California, 92093, USA*

We report the origin of the effect of nanoscale confinement on the local viscosity of entangled polystyrene (PS) films at temperatures far above the glass transition temperature. By using marker x-ray photon correlation spectroscopy with gold nanoparticles embedded in the PS films prepared on solid substrates, we have determined the local viscosity as a function of the distance from the polymer-substrate interface. The results show the impact of a very thin adsorbed layer (~ 7 nm in thickness) even without specific interactions of the polymer with the substrate, overcoming the effect of a surface mobile layer at the air-polymer interface and thereby resulting in a significant increase in the local viscosity as approaching the substrate interface.

It is well known that various properties of polymers confined on a nanometer length scale differ substantially from their bulk values. Most of the previous studies have focused on the glass transition temperature (T_g), which has been found to be reduced relative to that of the bulk since the original report by Keddie, Jones, and Cory [1]. Specifically, Torkelson and co-workers have shown that the decrease in T_g depends on the length scale over which perturbations to T_g originating at the air-polymer interface propagate into a film (the so-called "free-surface effect") [2–4]. In contrast to this concept, Napolitano *et al.* have recently reported that a very thin irreversibly adsorbed layer at the substrate interface is responsible for the T_g-confinement effect even for very weak polymer-substrate interaction systems [5,6]. Thus, the effects of these interfacial layers on polymer characteristics still remain a controversial area of research. One of the main reasons for this is due to the lack of experimental techniques that allow us to identify these interfacial layers in single nanoconfined polymer films simultaneously and to further decouple these interfacial effects as a function of the distance from the interfaces. In this Letter, we show that the irreversibly adsorbed layer plays a crucial role in determination of the local viscosity of entangled nanoconfined polystyrene (PS) films at temperatures far above the bulk T_g. We use x-ray photon correlation spectroscopy (XPCS) with gold nanoparticles as markers embedded in supported PS thin films, enabling us to measure the viscosity of polymer chains in the regions of interest [7]. The results reveal that while a surface mobile layer having reduced viscosity exists at the air-polymer interface, the long-range perturbations (~ 60 nm in thickness) associated with the irreversibly adsorbed layer formed onto the weakly interactive substrates result in the significant

increase in the viscosity with decreasing the distance from the substrate. Since the formation of the surface mobile layer [7–16] and irreversibly adsorbed layer [5,6,17–23] is rather general, the present experimental findings would shed new light on the impact of the irreversibly adsorbed layer on the local rheological property of polymer chains confined on a nanometer length scale.

Hydrogenated polystyrene (hPS, molecular weight (M_w) $= 123 \times 10^3$, Pressure Chemical Co.) with a narrow polydispersity ($M_w/M_n = 1.02$) was investigated. Thiol-functionalized [octadecanethiol ($C_{18}H_{37}SH$)] Au nanoparticles were prepared by using the one phase synthesis method [24]. The average radius of the Au particles was 1.5 ± 0.2 nm and the thickness of the $C_{18}H_{37}SH$ layer was approximated to be 1.3 nm [7]. A series of hPS/Au films (the volume fraction of the Au nanoparticles was fixed to be 0.2%) with four different thicknesses ($h = 32, 57, 128$ and 235 nm) were prepared onto hydrogen-passivated silicon (H-Si) substrates [25]. For the present study, all the films were annealed at 170 °C for 90 h under vacuum to ensure the equilibrium. According to a previous report [26], the index of refraction and the film thickness of spin cast PS thin films (thicknesses ranging from 13 nm to 130 nm) decreased by ~ 0.2 (measured by a spectroscopic ellipsometer equipped with a He-Ne laser) and ~ 2 nm, respectively, relative to those of the annealed films at $T = 160$ °C for 2 h after spin-coating. Therefore, we have defined the equilibrium time as the time when these parameters remain unchanged in the course of the annealing process. It is found that the annealing time of about 30 h at $T = 170$ °C is needed for the PS/Au thin films to achieve the equilibrium. In addition, it should be noted that this long annealing time is much longer than the "adsorption time" (~ 6.5 h for the PS/Au films used in
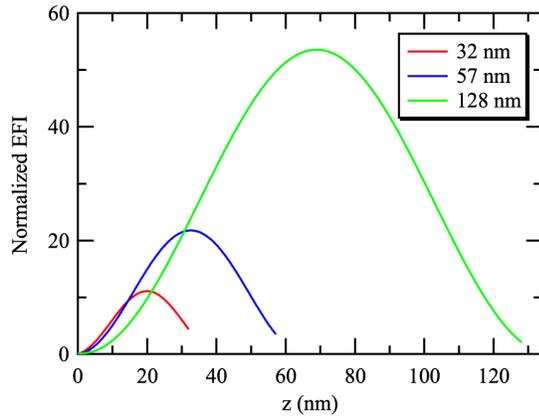
FIG. 1 (color online). Calculated REX EFI profiles in the center mode as a function of the distance (z) from the air-polymer interface for the three film thicknesses. The resonance intensity is normalized by the incident beam intensity.

FIG. 2 (color online). Measured g_2 functions for the 57 nm film (a) in the surface mode and (b) center mode at 156 °C. The solid lines are the best-fitted functions described in the text.

this study) which has been defined independently to reach a steady state for the conformation of polymer thin films [6]. We also confirmed that the Au particles were dispersed well in all the films before and after the XPCS experiments using transmission electron microscopy [7,25].

The marker XPCS experiments were performed at the beam line 8-ID at the Advanced Photon Source, Argonne National Laboratory. We have previously shown [7] that (i) the PS/Au system used in this study has the weak polymer-nanoparticle interaction whereby, the Brownian motion of the markers adequately tracks the viscosity of the polymer matrix via the Stokes-Einstein relationship and (ii) the marker motion is primarily probing entangled dynamics of polymer chains in the regions of interest, although the diameter of the Au nanoparticles (5.6 nm) is somewhat smaller than the tube diameter for entangled PS (about 9 nm) [27]. Hence, the marker XPCS technique enables us to measure the local viscosity of polymer chains governed by chain entanglements. In this study, we explore the *in situ* marker dynamics at the topmost surface and the rest of a film (preferentially the near-center region) independently by using the two illuminated modes with different incident angles (θ): (i) $\theta = 0.15°$, which is just below the critical angle (θ_c) of the total external reflection for PS ($\theta_c = 0.16°$ with x-ray energy of 7.5 keV used in this study) such that the electric field intensity (EFI) decays exponentially into the film and thereby scattering intensity is dominated by the surface area of about 9 nm [28]. We assign this experimental configuration as the "surface mode" hereafter. (ii) With the incident angle just above θ_c known as "the first resonance mode," [29] where resonance enhancement of the EFI in a polymer film takes place, and resonance-enhanced x-rays (REX) are intensified at the position close to the center of the film, as shown in Fig. 1. At the same time, scattering signals from the air-polymer interface can be completely eliminated (Fig. 1), improving the sensitivity of using REX to probe the
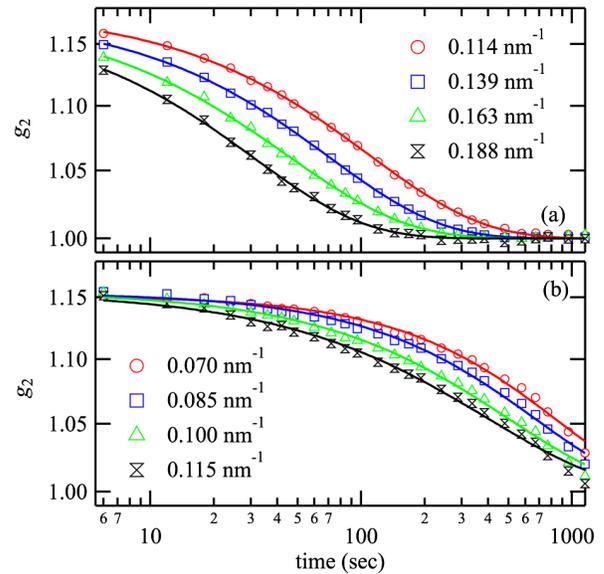
dynamics of the markers. We assign this experimental configuration as the "center mode" hereafter. XPCS measurements were made at temperatures of 156, 166, 176 and 186 °C under vacuum to avoid the effect of T_g on the dynamics.

Representative normalized intensity-intensity time auto-correlation (g_2) functions obtained at four different in-plane scattering vector ($q_\parallel$) values for the 57 nm thickness measured at 156 °C are shown in Fig. 2 [25]. All the experimental data for the 32 nm and 57 nm films could be fitted by stretched exponential decaying functions (i.e., $g_2(q_\parallel, t) = 1 + \exp[-2(t/\tau)^\alpha]$) with the range of $\alpha = 0.4$–0.8, where τ and α ($0 < \alpha < 1$) are the characteristic relaxation time and the stretching exponent that character-izes the shape, respectively. On the other hand, single exponential functions ($\alpha = 1$) were well fitted with all the g_2 functions for the 128 nm [7] and 235 nm films. As will be discussed later, the differences in α are attributed to the presence of heterogeneous environments within the two thinner films, thereby leading to a wider spectrum of relaxation times. Figure 3 shows the $q_\parallel$ dependences of τ for the 57 nm film at 186 °C where we can see the power-law behavior of $\tau \propto q_\parallel^{-2}$ for both modes, which is a char-acteristic of translational diffusive motions of particles and is true for all the temperatures used in this study. As shown in Fig. 3, the same power law can be seen in the surface mode for the 32 nm film, but the τ values are more than 2 orders of magnitude larger than those for the 57 nm film at the given temperatures. It should be noted that the marker dynamics in the center mode for the 32 nm film has been observed as well, but because the correlation times (~ 5000 s) are very close to the resolution of the
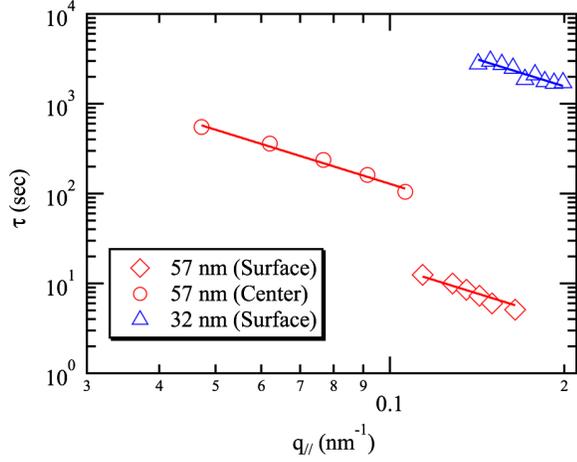
FIG. 3 (color online). Log-log plot of τ vs $q_\parallel$ for $h = 32$ nm and 57 nm in the surface mode and center mode at 186 °C. The solid lines correspond to the best fits of the power-law relationship of $\tau \propto q_\parallel^{-2}$ to the data.

measurements, quantitative analysis may not be appropriate. Although the relationship of $\tau = 1/2Dq_\parallel^2$, where D is the diffusion constant, is not strictly valid when the decay of a g_2 function is nonexponential, we use it for the purpose of comparison to other data. From the best fits to the data (the solid lines in Fig. 3) with the relationship, the "effective" D values for the surface mode (D_{sur}) and center mode (D_{cen}) are calculated. Table I summarizes the results along with the D values for the 128 nm and 235 nm films where the exponential decay is observed at both modes. From the table we can see that both D_{sur} and D_{cen} values for the 235 nm film are in good agreement with those for the 128 nm film where the difference in these D values is attributed to the reduced viscosity layer at the topmost surface at $T \gg T_g$ [7]. Despite some controversy, there is growing experimental evidence of a surface mobile layer [7–16] and recent simulations also support this concept [30]. Hence, our experimental results support these previous studies and further elucidate that the surface reduced viscosity layer exists regardless of film thickness (at least more than 57 nm in thickness) at $T \gg T_g$, as discussed below.

TABLE I. Measured diffusion coefficients of the Au nanoparticles and calculated viscosities based on the SE law at the surface and the near-center of the films at 186 °C.

h(nm)	D_{sur}(nm^2/s)	D_{cen}(nm^2/s)	η_{sur}(Ns/m^2)	η_{cen}(Ns/m^2)
32	0.016	-[a]	7.7×10^6	-[a]
57	6.58	0.76	1.8×10^4	1.6×10^5
128	7.80	5.30	1.5×10^4	2.2×10^4
235	7.84	5.42	1.5×10^4	2.2×10^4

[a]Ultraslow dynamics (the very weak $q_\parallel$ dependence of τ).

In order to explore the mechanism for the slowing dynamics of the markers embedded in the 32 and 57 nm films, we next focus on the substrate interface. According to a recent report [20], hPS thin films, which were spun cast on H-Si substrates and then annealed for several hours at 150 °C, showed a very thin residual layer even after thoroughly rinsing them with toluene (a good solvent for PS). In fact, our x-ray reflectivity experiments [25] have proved the presence of the residual layer of about 7 nm in thickness after rinsing all the hPS/Au films with toluene. Furthermore, by using neutron reflectivity, we have measured the interdiffusion process for a bilayer composed of deuterated PS (dPS, $M_w = 334 \times 10^3$, 51 nm in thick) floated onto the residual layer, giving the experimental evidence of no interdiffusion for at least 3 days at 170 °C [25]. Hence, these experimental results elucidate the existence of the very thin residual layer in which no dynamics of the polymer chains is favorable even at $T \gg T_g$.

Having attained the irreversibly adsorbed layer and established the surface reduced viscosity layer, we further illuminate the effects of the adsorbed layer that plays a dominant role in the slow dynamics. At the distance of approximately 20 nm from the substrate, which is intensified by the center mode for the 32 nm film, there is almost no dynamics of the markers within the time and wave vector domains used for XPCS. Since the irreversibly adsorbed layer is only 7 nm in thickness and the contribution to the total scattering signals obtained by the center-mode XPCS is a small portion (see Fig. 1), the ultraslow dynamics may not be directly linked to the adsorbed layer. Rather it would arise from the so-called "reduced mobility interface layer" [17,31,32], which would be entangled through the network of the adsorbed layer [33], thereby propagating the effect of the irreversibly adsorbed layer even at the distance over the coil size away from the substrate. In addition, as seen in the surface mode for the 32 nm film, the substrate effect propagates to the surface probed region thoroughly and overwhelms the effect of the surface reduced viscosity layer (if any), giving rise to the very small D_{sur} value (about 2 orders of magnitude smaller than those of the other thicker films, see Table I). Moreover, we should notice that the marker dynamics in the surface probed region of the 57 nm film is to some extent perturbed by the substrate effect as well, judging from the slight decrease in D_{sur} relative to D_{sur} for the 128 and 235 nm films (Table I). We shall discuss the critical threshold of the long-range perturbations later. It is also important to point out that the present results are quite different from the T_g distributions within PS thin films reported [2–4]: the surface enhanced layer with a large T_g reduction relative to the bulk mainly controls the distributions depending on the extent of nanoconfinement. Hence, the effect of T_g on the heterogeneous dynamics would be ruled out.

Then the question is what is the origin of the slow dynamics of the markers? As reported previously for PS thin films of about 130 nm in thickness [7], one might expect the dynamics of the markers embedded in the 57 nm film to follow the temperature dependence of the local viscosity in the probed regions, motivated by the Stokes-Einstein (SE) law, i.e., $D = k_B T/(6\pi R_E \eta)$, where k_B is the Boltzmann constant, T is the absolute temperature, and R_E is the effective radius of the Au nanoparticles. Figure 4 shows the temperature dependences of the effective local viscosity values at the surface (η_{sur}) and the near center (η_{cen}) for the 57 nm film calculated from the SE law with the calculated D values. At the same time, the "average" film viscosity (η_{cap}) of the hPS/Au film, which is independently determined from thermally driven capillary waves at the air-polymer interface using another XPCS mode ("capillary mode") [28], is also plotted for comparison. Using the normal hydrodynamic theory for capillary wave fluctuations on viscous (homogeneous) liquid films, Kim *et al.* have demonstrated that the film viscosity of single PS films, several tens of nanometers in thickness, is in good agreement with the bulk [28]. As seen in Fig. 4, the η_{sur} values are comparable to the η_{cap} values, while the η_{cen} values are by a factor of about 10 larger. The correspondence between the η_{sur} and η_{cap} values would support the recent experimental report [16] that the surface mobile layer can modify the overall dynamics of ultrathin PS supported films. In other words, this confirms that the marker dynamics in the 57 nm film also tracks the local viscosity reasonably. Moreover, we found that the η_{cap} values for the 57, 128, and 235 nm films remain constant

at all the temperatures used, indicating that the same surface mobile layer exists at the topmost surface of the three films. Given this and the somewhat perturbed marker dynamics at the surface of the 57 nm film, we may draw the conclusion that the long-range perturbations associated with the irreversibly adsorbed layer are limited to less than 57 nm from the substrate, resulting in the heterogeneous environment over the surface probed region of the 57 nm film and thereby the nonexponential decay of the g_2 functions [Fig. 2(a)].

The effective η_{sur} and η_{cen} values for each film at 186 °C are also summarized in Table I. Hence, we can see that the local viscosity in the different probed regions increases by at least 2 orders of magnitude with decreasing distance from the substrate interface, which is valid for all the temperatures. In order to interpret this phenomenon, we introduce previous interdiffusion experiments for PS multilayers where a labeled layer of dPS was placed in a matrix of hPS at varying distances from the H-Si substrate interface [34]. Zheng *et al.* have shown that the diffusion coefficient near the substrate is on the order of 100 times smaller than the bulk and is scaled as $N^{-3/2}$ (N is the degree of polymerization) compared to N^{-2} in the bulk. They conclude that this unusual scaling behavior can still be explained by the reptation theory [35] considering monomer-substrate contacts ($\sim N^{1/2}$ per chain) that restrict the chain mobility and modify the friction force from the bulk. Their model may be applicable here with the fact that the $N^{1/2}$ contacts are characteristic of the PS irreversibly adsorbed layer [20] and the viscosity of entangled polymer chains is inversely proportional to the diffusion coefficient [36]. However, more experimental and theoretical work needs to be done to validate the scaling behavior as well as chain entanglements in terms of the adsorbed layer.

Finally, the above results would remind us of the "percolation transition" in supercooled polymer thin films near T_g [37]. To estimate the local T_g, which may be different from the bulk, we utilized the temperature scaling of the local viscosity. The solid lines in Fig. 4 correspond to the best fits to the data with the Williams-Landel-Ferry (WLF) equation [38], $\log(\eta(T)/\eta(T_0)) = -c(T - T_0)/(T - T_\infty)$, where T_0 is a reference temperature chosen, c is a numerical constant, and T_∞ is a fixed temperature at which, regardless of the arbitrary choice of T_0, $\log(\eta(T)/\eta(T_0))$ being infinite. The best fits of the WLF equation to the data gave us $c = 4.0 \pm 0.5$ and $T_\infty = 48 \pm 2$ °C for η_{sur}, and $c = 4.0 \pm 0.5$ and $T_\infty = 65 \pm 2$ °C for η_{cen}, respectively. Hence the T_g values (50 °C above for PS [39]) at the surface and near center of the 57 nm film are bulklike (~ 100 °C) and 115 °C, respectively, while a slight decrease in T_g near the center of a supported PS film of about 60 nm thickness was reported by fluorescence label experiments [2]. Although the determination of the full distribution of the T_g values is beyond the scope of this
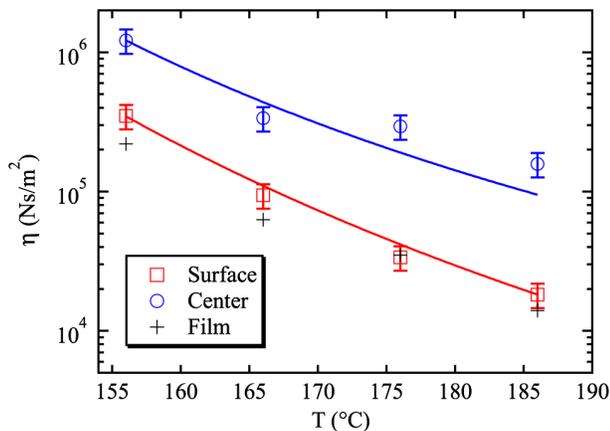

FIG. 4 (color online).   Temperature dependences of the local viscosity at the surface and near center of the 57 nm film. The average film viscosity determined from the thermally induced capillary fluctuations is also plotted (cross symbols). The solid lines correspond to the best fits of the WLF equation to the data with $c = 4.0 \pm 0.5$ and $T_\infty = 48 \pm 2$ °C for the surface mode, and $c = 4.0 \pm 0.5$ and $T_\infty = 65 \pm 2$ °C for the center mode, respectively.

study, it is reasonable to deduce that the phenomenon found in this study occurs at $T \gg T_g$.

The present Letter hence points to new physics in our understanding of the effect of confinements on the local viscosity of polymer chains: a very thin irreversibly adsorbed layer plays a vital role even without specific interactions of the polymer with the substrate interface, in contrast to the free-surface effect on T_g. This incongruity may lead to the important conclusion that the viscosity-confinement effect is not simply linked to the T_g-confinement effect. On the other hand, it is important to address that the critical threshold (~ 60 nm in thickness) for the long-range perturbations associated with the irreversibly adsorbed layer is in good agreement with that for the free-surface effect on T_g (~ 60 nm in thickness for supported PS films regardless of molecular weights [2,3,40]). Further XPCS experiments for different polymers (molecular weights and rigidity) and substrates will be carried out to illuminate generalities and/or differences between the viscosity-confinement effect and T_g-confinement effect, providing a better understanding of the global dynamics of polymer chains confined on a nanometer length scale.

*tkoga@notes.cc.sunysb.edu

[1] J. L. Keddie, R. A. L. Jones, and R. A. Cory, Europhys. Lett. **27**, 59 (1994).
[2] C. J. Ellison and J. M. Torkelson, Nature Mater. **2**, 695 (2003).
[3] C. J. Ellison, M. K. Mundra, and J. M. Torkelson, Macromolecules **38**, 1767 (2005).
[4] C. B. Roth et al., Macromolecules **40**, 2568 (2007).
[5] S. Napolitano et al., ACS Nano **4**, 841 (2010).
[6] S. Napolitano and M. Wübbenhorst, Nature Commun. **2**, 260 (2011).
[7] T. Koga et al., Phys. Rev. Lett. **104**, 066101 (2010).
[8] V. M. Rudoy et al., Colloid J. **64**, 746 (2002).
[9] J. H. Teichroeb and J. A. Forrest, Phys. Rev. Lett. **91**, 016104 (2003).
[10] P. Gasemjit and D. Johannsmann, J. Polym. Sci., Part B: Polym. Phys. **44**, 3031 (2006).
[11] R. M. Papaleo et al., Phys. Rev. B **74**, 094203 (2006).
[12] J. S. Sharp et al., Eur. Phys. J. E **22**, 287 (2007).
[13] D. Qi, Z. Fakhraai, and J. A. Forrest, Phys. Rev. Lett. **101**, 096101 (2008).
[14] Z. Fakhraai and J. A. Forrest, Science **319**, 600 (2008).
[15] M. Ilton, D. Qi, and J. A. Forrest, Macromolecules **42**, 6851 (2009).
[16] Z. Yang et al., Science **328**, 1676 (2010).
[17] S. Napolitano and M. Wübbenhorst, J. Phys. Chem. B **111**, 9197 (2007).
[18] S. Napolitano et al., Langmuir **23**, 2103 (2007).
[19] S. Napolitano, V. Lupascu, and M. Wübbenhorst, Macromolecules **41**, 1061 (2008).
[20] Y. Fujii et al., Macromolecules **42**, 7418 (2009).
[21] C. Rotella et al., Macromolecules **43**, 8686 (2010).
[22] C. Rotella, M. Wübbenhorst, and S. Napolitano, Soft Matter **7**, 5260 (2011).
[23] S. Napolitano, C. Rotella, and M. Wübbenhorst, Macromol. Rapid Commun. **32**, 844 (2011).
[24] C. K. Yee et al., Langmuir **15**, 3486 (1999).
[25] See Supplemental Material at http://link.aps.org/supplemental/10.1103/PhysRevLett.107.225901 for the details of the materials, methods, and NR results.
[26] X. Hu et al., High Performance Polymers **12**, 621 (2000).
[27] W. W. Graessley, J. Polym. Sci., Part B: Polym. Phys. **18**, 27 (1980).
[28] H. Kim et al., Phys. Rev. Lett. **90**, 068302 (2003).
[29] J. Wang, M. Bedzyk, and M. Caffrey, Science **258**, 775 (1992).
[30] S. Peter et al., J. Phys. Condens. Matter **19**, 205119 (2007).
[31] W. E. Wallace, J. H. van Zanten, and W. L. Wu, Phys. Rev. E **52**, R3329 (1995).
[32] J. H. van Zanten, W. E. Wallace, and W. L. Wu, Phys. Rev. E **53**, R2053 (1996).
[33] R. Bruinsma, Macromolecules **23**, 276 (1990).
[34] X. Zheng et al., Phys. Rev. Lett. **79**, 241 (1997).
[35] M. Doi and S. F. Edwards, The Theory of Polymer Dynamics (Oxford Science, Oxford, 1986).
[36] P. F. Green and E. J. Kramer, J. Mater. Res. **1**, 202 (1986).
[37] A. R. C. Baljon, J. Billen, and R. Khare, Phys. Rev. Lett. **93**, 255701 (2004).
[38] M. L. Williams, R. F. Landel, and J. D. Ferry, J. Am. Chem. Soc. **77**, 3701 (1955).
[39] J. D. Ferry, Viscoelastic Properties of Polymers (Wiley, New York, 1980).
[40] Z. Fakhraai and J. A. Forrest, Phys. Rev. Lett. **95**, 025701 (2005).